3432–3440 *Nucleic Acids Research, 2010, Vol. 38, No. 10* *Published online 2 February 2010*
doi:10.1093/nar/gkq036

The structure of DdrB from *Deinococcus*: a new fold for single-stranded DNA binding proteins

Seiji Sugiman-Marangos and Murray S. Junop*

Department of Biochemistry and Biomedical Sciences and M. G. DeGroote Institute for Infectious Disease Research, McMaster University, 1200 Main Street West, Hamilton, Ontario L8N 3Z5, Canada

Received November 9, 2009; Revised January 8, 2010; Accepted January 14, 2010

ABSTRACT

***Deinococcus* spp. are renowned for their amazing ability to recover rapidly from severe genomic fragmentation as a result of exposure to extreme levels of ionizing radiation or desiccation. Despite having been originally characterized over 50 years ago, the mechanism underlying this remarkable repair process is still poorly understood. Here, we report the 2.8 Å structure of DdrB, a single-stranded DNA (ssDNA) binding protein unique to *Deinococcus* spp. that is crucial for recovery following DNA damage. DdrB forms a pentameric ring capable of binding single-stranded but not double-stranded DNA. Unexpectedly, the crystal structure reveals that DdrB comprises a novel fold that is structurally and topologically distinct from all other single-stranded binding (SSB) proteins characterized to date. The need for a unique ssDNA binding function in response to severe damage, suggests a distinct role for DdrB which may encompass not only standard SSB protein function in protection of ssDNA, but also more specialized roles in protein recruitment or DNA architecture maintenance. Possible mechanisms of DdrB action in damage recovery are discussed.**

INTRODUCTION

Of the various types of damage that can occur within a cell, damage to genetic material in the form of DNA double-strand breaks (DSB) is particularly detrimental. A single unrepaired DSB is lethal to unicellular organisms such as *Escherichia coli*, while incorrect repair can lead to the loss of important genetic information, potentially resulting in chromosomal re-arrangement and cancer in higher organisms (1). *Deinococcus* spp. possess remarkable resilience to DNA damage. The model organism *D. radiodurans* is able to withstand ~15 000 Gy of γ-radiation, which effectively shatters the genome into hundreds of fragments (~20–30 kb) (2). Such a catastrophic event would be lethal several times over in the majority of terrestrial organisms, a lethal radiation dose in humans is in the range of 2–10 Gy, yet *D. radiodurans* is able to survive and accurately reassemble its genetic material in a matter of hours.

Since its discovery over 50 years ago (3), a number of mechanisms have been proposed to explain the extreme radiation resistance observed in *Deinococcus* spp. *Deinococcus radiodurans* does not prevent formation of DSBs and is observed to accumulate damage at the same rate as other, non-radiation resistant bacteria. Resistance to extreme ionizing radiation (IR) is thought to result from a combination of efficient protection of repair proteins by Mn^{2+}-dependent ROS scavengers (2,4,5) and a robust repair pathway reliant on proteins unique to *Deinococcus* spp. (2,6–8).

Repair in *D. radiodurans* that occurs in response to severe IR exposure takes place in a two-stage process. The first stage, termed Extended Synthesis Dependent Strand Annealing (ESDSA), involves the formation of >20-kb long 3′ single-stranded DNA (ssDNA) extensions. These unusual structures result from successive rounds of strand invasion of homologous fragments followed by Pol I- and Pol III-mediated extension (2,7). Exceptionally, long stretches of ssDNA generated by this process must be protected from degradation, non-specific annealing and self-association so that they can be efficiently converted into linear duplex DNA in the final stage of ESDSA. In the second stage of repair, long linear DNA molecules generated by ESDSA are pieced together to generate complete circular chromosomes via RecA-dependent homologous recombination.

Damage recovery is also dependent on *de novo* protein synthesis (9). Microarray hybridization studies identified a small subset of *Deinococcus* spp.-specific genes that are highly up-regulated in response to extreme IR exposure and necessary for recovery (8,10). Of the proteins identified, DNA damage response B (DdrB) is perhaps the most intriguing. In *D. radiodurans*, *ddrB* (DR0070) experiences a >40-fold induction immediately following exposure to 3 kGy of γ-radiation, while a Δ*ddrB* strain

*To whom correspondence should be addressed. Tel: +1 905 525 9140 (extn: 22912); Fax: +1 905 522 9033; Email: junopm@mcmaster.ca

experiences a 100-fold decrease in viability with respect to the wild-type strain following exposure to 10 kGy (8). In addition to being highly up-regulated and of obvious importance to damage recovery, DdrB is conserved within and unique to *Deinococcus* spp.

Recently, it was reported that DdrB may represent a member of a new family of bacterial single-stranded binding (SSB) protein (11). SSBs are essential proteins found in organisms from all domains of life, which play an important role in DNA metabolism, replication, recombination and repair (12). Each of these processes generate ssDNA, which has the tendency to form secondary structures and is susceptible to non-specific cleavage by rogue nucleases. SSBs protect and stabilize exposed ssDNA by wrapping the nucleic acid strand around a conserved flattened face of a 5-stranded β-barrel structure, known as an oligonucleotide-binding (OB) fold (12). Single strand DNA makes multiple non-contiguous contacts with each monomer within a SSB tetramer (31). This mode of binding efficiently compacts ssDNA into a highly intertwined complex. SSBs also act as a recruiting scaffold for targeting other proteins and protein complexes to the site of action (12). Considering the importance of SSB function in protecting the hundreds of >20 kb ssDNA fragments generated during ESDSA, it is surprising that even under the stresses of massive DNA damage, *ssb* in *D. radiodurans* only experiences a slight increase in expression (~3-fold) (10). Under the same conditions, *ddrB* expression is increased >40-fold, suggesting that it may substitute for SSB during damage recovery (8). If DdrB is in fact an alternative SSB, unique to *Deinococcus* spp., it may serve to recruit a distinct set of proteins necessary for recovery from extreme IR exposure.

To date, all SSB homologues that have been characterized interact with their ssDNA substrates by means of a structurally conserved OB domain (12). In this article, we report the X-ray crystal structure of DdrB from *D. geothermalis* to 2.8 Å resolution. Unexpectedly, DdrB was found to contain a novel ssDNA-binding fold, which is structurally and topologically distinct from the OB-fold. DdrB, therefore represents the founding member of a new class of SSBs that lack the otherwise universal OB-domain.

MATERIALS AND METHODS

Protein expression and purification

DdrB (Dgeo_0070) from *D. geothermalis* was cloned into the pET151-D-topo vector (Invitrogen) according to the manufacturer's protocol and expressed in *E. coli* BL21(DE3) as an N-terminal hexa-histidine (6His) tagged protein. Cultures were grown at 37°C to an OD_{600} of ~0.5 and induced with 1 mM isopropyl β-D-thiogalactopyranoside (IPTG) for 3 h. DdrB labeled with SeMet was expressed in the methionine auxotrophic strain *E. coli* B834 using SeMet M9 media from Shanghai Medicilon Inc. (http://www.medicilonic.com). DdrB-SeMet was expressed in the same manner as wild-type DdrB except that the cells were induced with IPTG when the OD_{600} reached ~1.2. Cell pellets of both native and SeMet DdrB were resuspended in lysis buffer (20 mM Tris pH 8.0, 1 M NaCl, 5 mM imidazole) and lysed by sonication. Following clarification by centrifugation at 48 000*g*, soluble lysate was loaded onto a 5 ml Ni-IMAC column at 1 ml/min using an AKTA FPLC. The bound protein was washed with 5 column volumes of wash buffer (105 mM imidazole) prior to elution (250 mM imidazole). Ni-IMAC column eluate was exchanged into low salt buffer (20 mM Tris pH 8.0, 150 mM KCl) prior to cleavage of the 6His tag with TEV protease. Uncleaved fusion, cleaved 6His tag and TEV were separated from the cleaved DdrB by passing the TEV digestion mixture over the 5 ml Ni-IMAC column. Pure, untagged DdrB was collected in the flow through fraction (Supplementary Figure S3).

Electrophoretic mobility shift assay

Nucleic acid binding experiments were performed in electrophoretic mobility shift assay (EMSA) buffer (20 mM Tris pH 8.0, 150 mM NaCl, 10% glycerol) by mixing 150 pmol of 20b ssDNA, 20bp dsDNA or 20b ssRNA for 15 min with increasing amounts of DdrB (100, 250, 500, 1000 pmol). The reactions were resolved by electrophoresis on a 10% polyacrylamide native TBE gel running at 80 V for 1 h.

Structure determination of DdrB

All DdrB crystals were grown at 20°C using the hanging-drop vapor diffusion method. Equal volumes (1 μl) of native DdrB (24.7 mg/ml) and crystallization solution (0.1 M sodium acetate anhydrous pH 4.6, 2 M ammonium sulfate) were mixed and dehydrated over 0.5 ml 1.5 M ammonium sulfate. SeMet DdrB (25 mg/ml) was mixed with an equal volume (3 μl) of crystallization solution [0.1 M sodium acetate anhydrous pH 5.5, 2.45 M ammonium sulfate, 0.01 M Praseodymium(III) acetate hydrate] and dehydrated against 0.5 ml 1.5 M ammonium sulfate. DdrB-SeMet crystals were transferred into cryogenic buffer (0.1 M trisodium citrate dehydrate pH 5.6, 20% isopropanol, 20% PEG 4000) prior to flash cooling in a nitrogen stream. A single-wavelength anamolous diffraction (SAD) data set was collected at a wavelength of 0.979 Å on the X26C beamline of the National Synchrotron Light Source at Brookhaven National Laboratory. The data set was processed and scaled with HKL2000 (13) to 2.8 Å. Of the 15 expected SeMet sites, 10 were located using Phenix-AutoSol (14). Phasing and density modification carried out with the Phenix software package was used to generate an experimental map. Model building and refinement of the DdrB structure was carried out through multiple iterations of Coot (15) and Phenix-Refine until R and R_{free} values converged and geometry statistics reached suitable ranges.

Surface area calculations to determine the extent of protein–protein interaction surfaces were performed by AreaIMol (16,17). Least squares analysis to determine the structural similarity between regions of DdrB and SSB was carried out using LSQKAB (18).

RESULTS AND DISCUSSION

DdrB from *D. geothermalis* binds ssDNA but not dsDNA

We have performed EMSAs to assess *D. geothermalis* DdrB's ($DdrB_{Dg}$) nucleic acid binding capabilities with ss and dsDNA as well as ssRNA (Figure 1). $DdrB_{Dg}$ shifted a 20b ssDNA substrate, but failed to bind 20bp duplex DNA even at the highest protein concentration tested (Figure 1), suggesting that $DdrB_{Dg}$ is specific for its ability to interact stably with ss but not dsDNA. From this analysis, it would appear that $DdrB_{Dg}$ binds ssDNA with an affinity in the low μM range (<20 μM), comparable to other characterized SSBs (11,19).

Analysis of the $DdrB_{Dg}$:DNA ratios used in this study suggests that approximately 1 molecule of $DdrB_{Dg}$ is bound for every 5 nt of DNA substrate. When a 40-nt substrate was used this value increased to 10 nt per $DdrB_{Dg}$ monomer (Supplementary Figure S1), similar to findings for DdrB from *D. radiodurans* ($DdrB_{Dr}$) (11). $DdrB_{Dg}$ and $DdrB_{Dr}$ are 72% identical by primary amino acid sequence and therefore would be expected to display similar DNA binding characteristics. Both $DdrB_{Dg}$ and $DdrB_{Dr}$ were also found to associate weakly with ssRNA (Figure 1) (11). At this time the biological significance, if any, of this interaction is unclear. It will be interesting, however, to determine if DdrB-RNA binding plays a role in the ability of *Deinococcus* to recover from extreme DNA damage.

The crystal structure of DdrB from *D. geothermalis*

DdrB is a ssDNA binding protein that exhibits no primary sequence similarity to any other SSB characterized to date. This raises the possibility that DdrB may represent a new structural motif for ssDNA binding. By determining its crystal structure, we hoped to answer the question of whether DdrB is a distantly related homolog of the standard SSB, or a structurally distinct protein that has arisen to perform a specialized function in *Deinococcus* spp. The structure of DdrB was solved by SAD phasing using a 2.8 Å dataset collected from Selenomethionine (SeMet) derivatized protein. DdrB crystallized in the space group $P3_2$ and contained five monomers in the asymmetric unit. In our model, the main chain spans amino acid residues 1–126 in chains A and B, 1–127 in chains D and E and 1–129 in chain C, while full-length DdrB is 178 amino acid residues in length (discussed below). The final model was refined to R and R_{free} statistics of 23.5% and 28.5%, respectively. A complete list of X-ray diffraction data and model refinement statistics are given in Table 1.

The DdrB monomer (Figure 2) consists of an *N*-terminal β–β–α motif followed by a six-stranded

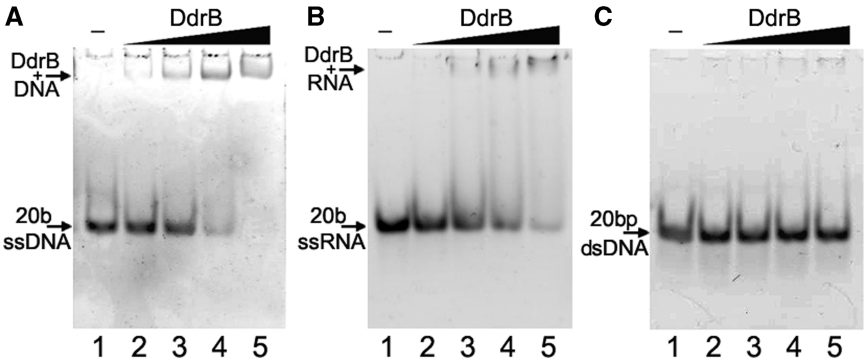

Figure 1. Electrophoretic mobility shift assay of ssDNA, ssRNA and dsDNA by DdrB. A total of 150 pmol of (**A**) 20b ssDNA, (**B**) 20b ssRNA and (**C**) 20bp dsDNA substrates were incubated with 100 (lane 2), 250 (lane 3), 500 (lane 4) and 1000 (lane 5) pmol of DdrB and resolved by 10% polyacrylamide native TBE gel electrophoresis. DdrB bound ssDNA but not dsDNA.

Table 1. Data collection and model refinement statistics

Data collection		Model and refinement	
Space group	$P3_2$	Resolution (Å)[a]	35.24–2.80
Cell parameters		R_{work}/R_{free} (%)	23.5/28.5
a, *b*, *c* (Å)	102.9, 102.9, 96.7	$Reflections_{observed}$	27 742
α, β, γ (°)	90, 90, 120	Reflections R_{free}	1867
Molecules in ASU	5	No. of atoms	
Resolution (Å)[a]	50.0–2.80	Protein	4715
Unique reflections	28 588	Ligand/ion	0
Redundancy[a]	9.9 (9.9)	Water	34
Completeness (%)[a]	99.9 (100.0)	R.m.s.d. bond	
I/σ(I)[a]	17.4 (3.7)	Lengths (Å)	0.013
R_{merge} (%)[a]	9.6 (42.3)	Angles (°)	1.63
Wilson B Factor (Å^2)	89.8	Average B Factor (Å^2)	97.4
		PDB Accession Code	3KDV

[a]Statistics for the highest resolution shell are shown in parentheses.

β-sheet (β3–β8–β7–β6–β5–β4) of which one face is solvent exposed and the other is packed against the N-terminal motif. Loop regions joining β6 to β7, and β7 to β8 are poorly ordered, leading to missing residues in both of these regions as well as little to no density for the majority of the side chains, suggesting that these are flexible regions of the protein with high tendency towards disorder.

The five monomers in the asymmetric unit are arranged in a ring-structure with a 10 Å solvent accessible pore running through the middle (Figure 3). The central pore is comprised of a 10-stranded anti-parallel β-barrel that is stabilized primarily through interactions of DdrB's N-terminal β–β–α motif. Protein–protein interactions within the pentamer bury ~30% of the total solvent-accessible area of each monomer (1991 Å^2), suggesting that the pentamer is a very stable structure. The formation of this pentameric structure was demonstrated in solution by gel-filtration experiments and is consistent with analytical ultracentrifugation studies performed with $DdrB_{Dr}$ (11).

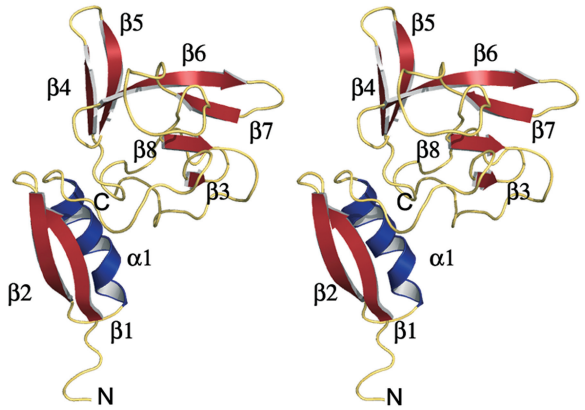

Figure 2. Stereo image of a DdrB (1-127) monomer. Secondary elements are colored as follows, α-helices in blue and β-strands in red.

The C-terminal region of DdrB

Analysis of the primary amino acid sequence of DdrB using the PSIpred server (20,21) predicts the C-terminal 35 residues of the protein as disordered. This is consistent with our observation that the final 51 residues of DdrB are unable to be assigned due to a lack of electron density, suggesting a high degree of mobility in this region of the protein. It does not, however, discount the potential importance. A BLAST (22) search using $DdrB_{Dg}$ as a query sequence, returned a related sequence within *D. geothermalis* (*Dgeo_2983*) that is predicted to encode an 83 amino acid protein sharing 72% similarity and 63% identity to the C-terminal region of $DdrB_{Dg}$ (Supplementary Figure S2). Although the function of this hypothetical protein is unknown, its existence gives support to the idea that the C-terminal region of DdrB may form a functional domain.

Interestingly, the latter region (~60 residues) of SSBs is also disordered (23) and has been shown to be essential for mediating protein–protein interactions via a conserved patch of C-terminal negatively charged residues (24). It is not uncommon for such clusters of charged amino

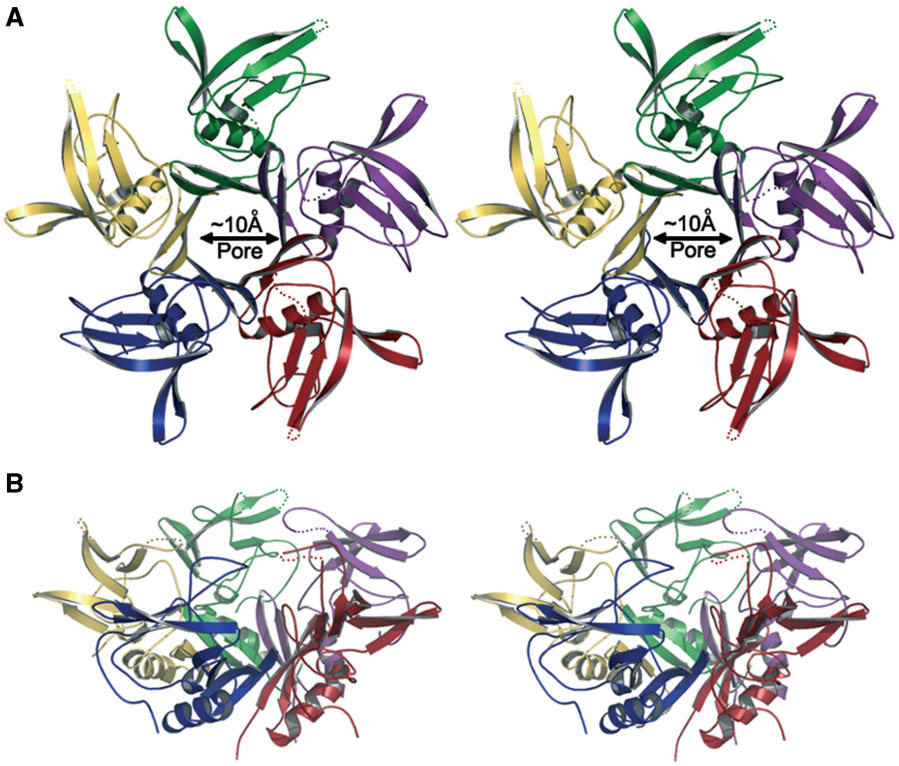

Figure 3. Stereo image of DdrB pentamer colored by chain (A, red; B, green; C, blue; D, yellow; E, purple). (**A**) View of 'top' face of the pentamer displaying the 10 Å central pore. (**B**) 'Side' view of the pentamer. Missing loop segments are represented by dotted lines.

acids to be involved in mediating protein–protein interactions (25). DdrB possesses several highly conserved charged residues within its last 50 amino acids, including a negative patch of residues directly at its C-terminus (Supplementary Figure S2). It is, therefore, quite possible that the C-terminus of DdrB behaves in a similar way as SSB, mediating interactions with other proteins important for DNA damage recovery.

Structure-based comparison of DdrB and OB-fold ssDNA binding proteins

To date, all SSB homologues have been shown to interact with ssDNA through a conserved OB-fold (12). The OB-fold is characterized by a pair of three-stranded anti-parallel β-sheets (β1–β2–β3 and β5–β4–β1) that form a five-stranded β-barrel (26). Strand β1 contributes to both sheets due to a conserved glycine residue close to its N-terminal end, and a β-bulge in the latter portion of the strand. All OB-fold proteins adopt a Greek key motif in the arrangement of the strands that contribute to the β5–β4–β1–β2–β3–barrel (Figure 4—SSB and DnaE) (26).

It was originally thought that DdrB may possess an OB-fold domain similar to those found in SSB and DNA polymerase III α-subunit (DnaE) (11). Searches performed using the structure of DdrB as query with the iCOPS (27), DALI (28), 3D-BLAST (29) and MATRAS (30) servers did not identify any OB-fold proteins as structural homologues. In fact, these standard homology searches did not yield any matches from the current structural databases, indicating that DdrB has a unique structure and fold not previously observed. Although the secondary-structure matching (SSM) superposition algorithm in Coot was not able to align DdrB with either *E. coli* SSB (SSB_{Ec}) (31) or *T. aquaticus* DnaE (32), we were able to perform a manual structural alignment in which the C_α-chains of four of the β-strands are in a similar spatial orientation (Figure 4). C_α carbons from DdrB $\beta4_{64–68}$, $\beta5_{71–77}$, $\beta6_{80–87}$ and $\beta7_{91–95}$ superimpose onto SSB_{Ec} $\beta4_{82–86}$, $\beta5_{97–103}$, $\beta3_{59–52}$ and $\beta2_{37–33}$ with root mean-squared deviations (RMSD) of 1.02, 0.87, 1.34 and 1.93 Å, respectively. Despite the very obvious and distinct structural similarities apparent between DdrB and the two OB-fold proteins, there are a number of features that clearly differentiate DdrB from the canonical OB-family. First, the β-sheet (excluding β3) adopts an up-and-down structural topology, rather than the Greek key motif that is conserved within the OB-fold (Figure 4). Second, the strands that display structural similarity between DdrB and SSB_{Ec} do not show similar topology, connectivity or directionality. Finally, Ddrb's β-sheet does not form a β-barrel and none of its strands possess the conserved glycine or β-bulge that permit the OB-fold β1 to contribute to multiple β-sheets. Taken together, it is evident that DdrB represents a new subfamily member of the OB-fold superfamily, as it possesses a unique architecture that is in all likelihood evolutionarily distinct from SSB_{Ec} and other members of the canonical OB-family.

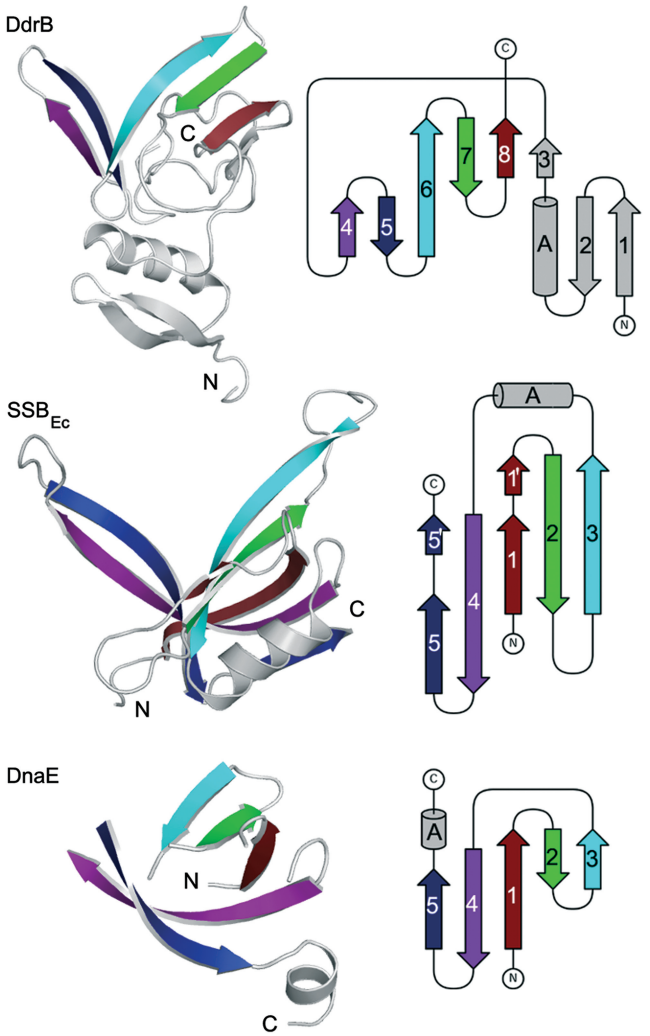

Figure 4. Structural comparison of DdrB (PDB: 3KDV), SSB_{Ec} (PDB: 1EYG) and DnaE (PDB: 2HPM). Structurally analogous strands are color coded on the structures and topology diagrams; unrelated segments are colored in gray.

Analogous ssDNA binding surfaces of DdrB and SSB_{Ec}

Alpha hemolysin, hexameric helicases such as *T7* gp4, *E. coli* RuvB and *Papillomavirus* E1, and sliding clamp proteins such as PCNA and *E. coli* β all form closed-ring structures that are able to thread DNA through their central pores. The central pore of DdrB's, however, is unlikely to bind DNA in a similar fashion. First, it has a very small (~10 Å) diameter compared to other ring-forming proteins known to associate with ssDNA, which are typically in the range of 14–40 Å (33–36). Secondly, the electrostatic surface potential of the pore carries a net negative charge (Figure 5), making it unfavorable for DNA association.

It would appear that despite structural differences, DdrB and SSB_{Ec} maintain similar DNA binding surfaces. In the crystal structure, SSB_{Ec} is observed to interact with DNA primarily via electrostatic and base-stacking interactions mediated by residues lying on the solvent exposed faces of β3, β4 and β5. Both positively charged and aromatic hydrophobic amino acids are

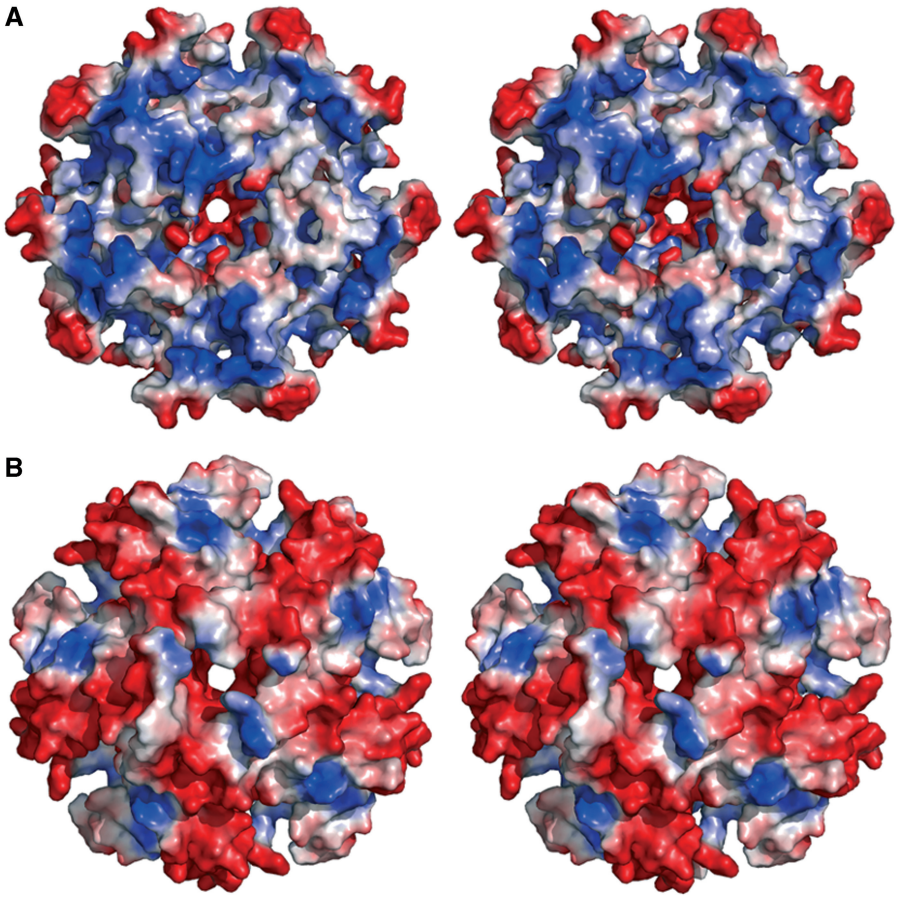

Figure 5. Stereo image of surface representation of the DdrB pentamer. (**A**) 'Top' face. (**B**) 'Bottom' face. Positive and negative electrostatic charge potentials are represented in blue and red, respectively.

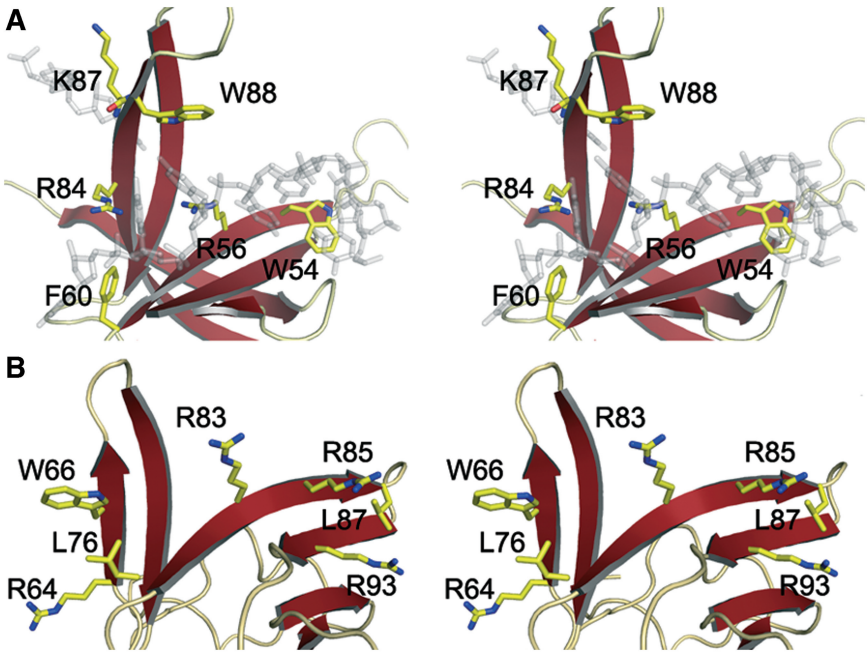

Figure 6. Stereo image of the conserved amino acid residues lining the solvent exposed DNA binding β-sheet surface of SSB_{Ec} (**A**) and the analogous surface of DdrB (**B**). Bound ssDNA is represented in gray to delineate the DNA binding surface of SSB_{Ec} (PDB: 1EYG).

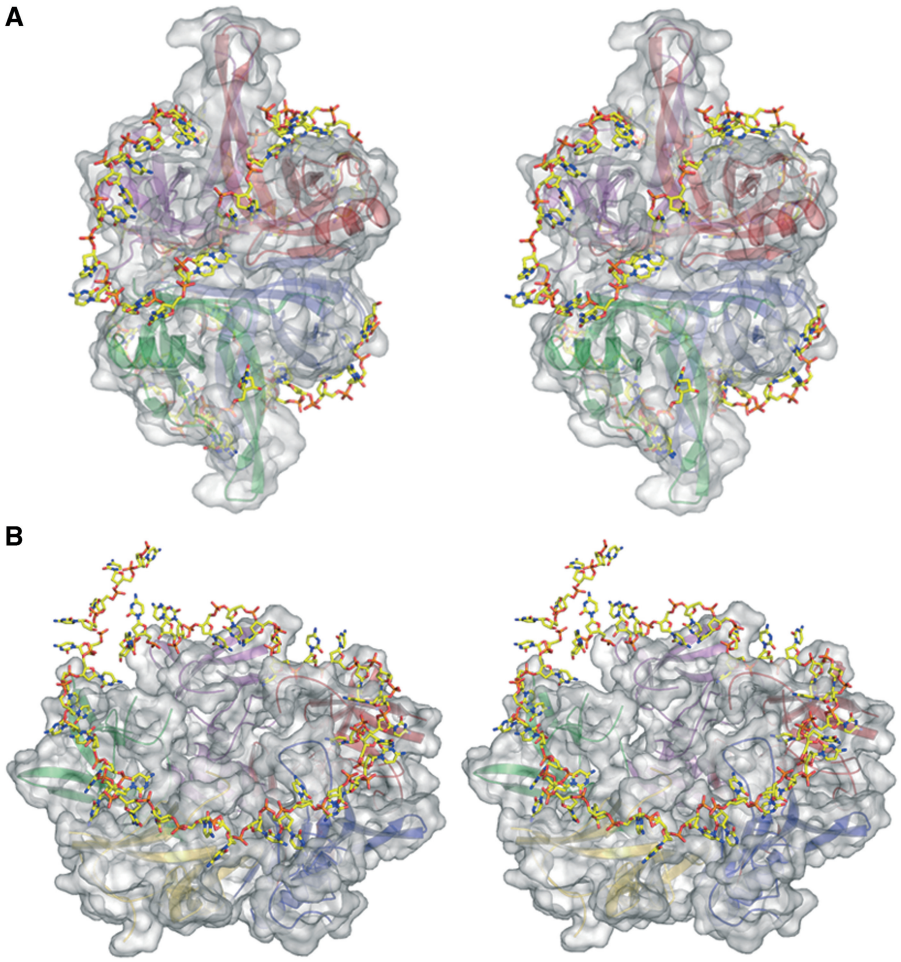

Figure 7. Stereo image of surface/cartoon representations of quaternary structures of SSB_{Ec} (PDB: 1EYG) and DdrB (PDB: 3KDV). Surfaces are represented in gray, and bound ssDNA is represented in stick form. (**A**) SSB_{EC} tetramer colored by chain (A,green; B, blue; C, red; D, purple) bound to two 35-mers of ssDNA. (**B**) DdrB pentamer colored by chain (A, red; B, green; C, blue; D, yellow; E, purple). A 40-mer of ssDNA is modeled onto the positively charged surface of the DdrB pentamer.

important for this DNA interaction (Figure 6A) (31). The only positively charged surface on DdrB corresponds to the solvent exposed face of the six-stranded beta sheet (Figure 5) that precisely aligns to the segments of SSB_{Ec} that display structural similarity (Figure 4). This surface contains a number of conserved charged, aromatic and hydrophobic residues able to fulfill the necessary interactions with ssDNA (Figure 6B).

The quaternary structures of DdrB (pentameric ring) and SSB_{Ec} (dimer of dimers) are very different, suggesting that their overall modes of DNA association may also be distinct. SSB_{Ec} binds ssDNA in a serpentine fashion with a single DNA molecule making multiple non-contiguous contacts with each monomer in a tetramer (Figure 7A). This type of binding efficiently compacts ssDNA into a highly intertwined complex. The pentameric ring structure of DdrB, however, has its DNA binding surfaces positioned such that intertwining of DNA is not possible. Rather, the quaternary structure of DdrB is more consistent with a simple contiguous wrapping mode for ssDNA binding analogous to the tire on the rim of a wheel (Figure 7B). Without a crystal structure, it is difficult to expand further; however, even from this simple comparison, it is apparent that the mechanisms for DNA binding are very different, reflecting the unique roles these proteins play in DNA metabolism.

The role of an alternative, DNA damage-inducible SSB

Standard bacterial SSB is expressed continuously and plays an essential role in stabilizing and protecting exposed ssDNA throughout regular cellular processes (12). During ESDSA repair following extreme DNA damage, immense spans of ssDNA totaling hundreds of kilobase pairs are generated (2); however, SSB expression is only moderately elevated (10). DdrB, on the other hand, is present at almost undetectable levels under regular growth conditions, but is among the top five most highly up-regulated genes under the stresses of excessive DNA damage (8). In addition to its role in protecting exposed ssDNA, SSB acts as a scaffolding protein able to recruit a variety of proteins during different cellular processes. As repair from extreme damage appears to involve a more diverse set of proteins and protein-complexes than simple DSB repair, DdrB may function as a specialized

SSB reserved exclusively for use in ESDSA. The discovery of a new SSB-like protein in *Deinococcus* spp. opens the question of whether additional specialized SSB-like proteins may also exist in other organisms that have missed being identified due to sequence and structural diversity.

ACCESSION NUMBER

The structure factor amplitudes and the refined coordinates of DdrB have been deposited in the Protein Data Bank as entry 3KDV.

SUPPLEMENTARY DATA

Supplementary Data are available at NAR Online.

ACKNOWLEDGEMENTS

Structural data was collected at the National Synchrotron Light Source, Brookhaven National Laboratories, at Beamlines X26C. We would like to thank Annie Héroux, Alexei Soares and Robert Sweet for their technical assistance. We also wish to thank Elena Gaidamakova for providing us with *D. geothermalis*.

FUNDING

Natural Sciences and Engineering Research Council of Canada grant (2008R00075 to M.S.J.); studentship (to S.N.S.M.). Funding for open access charge: Natural Sciences and Engineering Research Council of Canada.

Conflict of interest statement. None declared.

REFERENCES

1. Pardo,B., Gomez-Gonzalez,B. and Aguilera,A. (2009) DNA repair in mammalian cells: DNA double-strand break repair: How to fix a broken relationship. *Cell Mol. Life Sci.*, **66**, 1039–1056.
2. Zahradka,K., Slade,D., Bailone,A., Sommer,S., Averbeck,D., Petranovic,M., Lindner,A.B. and Radman,M. (2006) Reassembly of shattered chromosomes in *Deinococcus radiodurans*. *Nature*, **443**, 569–573.
3. Anderson,A.W., Nordan,H.C., Cain,R.F., Parish,G. and Duggan,D. (1956) Studies on a radioresistant Micrococcus. I. Isolation, morphology, cultural characteristics and resistance to gamma radiation. *Food Technol.*, **10**, 575–578.
4. Daly,M.J., Gaidamakova,E.K., Matrosova,V.Y., Vasilenko,A., Zhai,M., Venkateswaran,A., Hess,M., Omelchenko,M.V., Kostandarithes,H.M., Makarova,K.S. *et al.* (2004) Accumulation of Mn(II) in *Deinococcus radiodurans* facilitates gamma-radiation resistance. *Science*, **306**, 1025–1028.
5. Daly,M.J., Gaidamakova,E.K., Matrosova,V.Y., Vasilenko,A., Zhai,M., Leapman,R.D., Lai,B., Ravel,B., Li,S.M., Kemner,K.M. *et al.* (2007) Protein oxidation implicated as the primary determinant of bacterial radioresistance. *PLoS Biol.*, **5**, e92.
6. Makarova,K.S., Omelchenko,M.V., Gaidamakova,E.K., Matrosova,V.Y., Vasilenko,A., Zhai,M., Lapidus,A., Copeland,A., Kim,E., Land,M. *et al.* (2007) *Deinococcus geothermalis*: the pool of extreme radiation resistance genes shrinks. *PLoS ONE*, **2**, e955.
7. Slade,D., Lindner,A.B., Paul,G. and Radman,M. (2009) Recombination and replication in DNA repair of heavily irradiated *Deinococcus radiodurans*. *Cell*, **136**, 1044–1055.
8. Tanaka,M., Earl,A.M., Howell,H.A., Park,M.J., Eisen,J.A., Peterson,S.N. and Battista,J.R. (2004) Analysis of *Deinococcus radiodurans's* transcriptional response to ionizing radiation and desiccation reveals novel proteins that contribute to extreme radioresistance. *Genetics*, **168**, 21–33.
9. Dean,C.J., Little,J.G. and Serianni,R.W. (1970) The control of post irradiation DNA breakdown in *Micrococcus radiodurans*. *Biochem. Biophys. Res. Commun.*, **39**, 126–134.
10. Liu,Y., Zhou,J., Omelchenko,M.V., Beliaev,A.S., Venkateswaran,A., Stair,J., Wu,L., Thompson,D.K., Xu,D., Rogozin,I.B. *et al.* (2003) Transcriptome dynamics of *Deinococcus radiodurans* recovering from ionizing radiation. *Proc. Natl Acad. Sci. USA*, **100**, 4191–4196.
11. Norais,C.A., Chitteni-Pattu,S., Wood,E.A., Inman,R.B. and Cox,M.M. (2009) DdrB protein, an alternative *Deinococcus radiodurans* SSB induced by ionizing radiation. *J. Biol. Chem.*, **284**, 21402–21411.
12. Pestryakov,P.E. and Lavrik,O.I. (2008) Mechanisms of single-stranded DNA-binding protein functioning in cellular DNA metabolism. *Biochemistry*, **73**, 1388–1404.
13. Otwinowski,Z. and Minor,W. (1997) Processing of X-ray diffraction data collected in oscillation mode. In Carter,C.W.J. and Sweet,R.M. (eds), *Methods in Enzymology: Macromolecular Crystallography, Part A*, Vol. 276. Academic Press, New York, pp. 307–326.
14. Adams,P.D., Grosse-Kunstleve,R.W., Hung,L.W., Ioerger,T.R., McCoy,A.J., Moriarty,N.W., Read,R.J., Sacchettini,J.C., Sauter,N.K. and Terwilliger,T.C. (2002) PHENIX: Building new software for automated crystallographic structure determination. *Acta Crystallogr. D Biol. Crystallogr.*, **58**, 1948–1954.
15. Emsley,P. and Cowtan,K. (2004) Coot: model-building tools for molecular graphics. *Acta Crystallogr. D Biol. Crystallogr.*, **60**, 2126–2132.
16. Lee,B. and Richards,F.M. (1971) The interpretation of protein structures: estimation of static accessibility. *J. Mol. Biol.*, **55**, 379–400.
17. Saff,E. and Kuijlaars,A. (1997) Distributing many points on a sphere. *Math. Intell.*, **19**, 5–11.
18. Kabsch,W. (1976) A solution for the best rotation to relate two sets of vectors. *Acta Crystallogr. A*, **32**, 922–923.
19. Weiner,J.H., Bertsch,L.L. and Kornberg,A. (1975) The deoxyribonucleic acid unwinding protein of *Escherichia coli*. Properties and functions in replication. *J. Biol. Chem.*, **250**, 1972–1980.
20. Jones,D.T. (1999) Protein secondary structure prediction based on position-specific scoring matrices. *J. Mol. Biol.*, **292**, 195–202.
21. McGuffin,L.J., Bryson,K. and Jones,D.T. (2000) The PSIPRED protein structure prediction server. *Bioinformatics*, **16**, 404–405.
22. Altschul,S.F., Gish,W., Miller,W., Myers,E.W. and Lipman,D.J. (1990) Basic local alignment search tool. *J. Mol. Biol.*, **215**, 403–410.
23. Sancar,A., Williams,K.R., Chase,J.W. and Rupp,W.D. (1981) Sequences of the SSB gene and protein. *Proc. Natl Acad. Sci. USA*, **78**, 4274–4278.
24. Curth,U., Genschel,J., Urbanke,C. and Greipel,J. (1996) *In vitro* and *in vivo* function of the C-terminus of *Escherichia coli* single-stranded DNA binding protein. *Nucleic Acids Res.*, **24**, 2706–2711.
25. Zhu,Z.Y. and Karlin,S. (1996) Clusters of charged residues in protein three-dimensional structures. *Proc. Natl Acad. Sci. USA*, **93**, 8350–8355.
26. Theobald,D.L., Mitton-Fry,R.M. and Wuttke,D.S. (2003) Nucleic acid recognition by OB-fold proteins. *Annu. Rev. Biophys. Biomol. Struct.*, **32**, 115–133.
27. Suhrer,S.J., Wiederstein,M., Gruber,M. and Sippl,M.J. (2009) COPS—a novel workbench for explorations in fold space. *Nucleic Acids Res.*, **37**, W539–W544.
28. Holm,L., Kaariainen,S., Rosenstrom,P. and Schenkel,A. (2008) Searching protein structure databases with DaliLite v.3. *Bioinformatics*, **24**, 2780–2781.
29. Yang,J.M. and Tung,C.H. (2006) Protein structure database search and evolutionary classification. *Nucleic Acids Res.*, **34**, 3646–3659.

30. Kawabata,T. (2003) MATRAS: a program for protein 3D structure comparison. *Nucleic Acids Res*., **31**, 3367–3369.
31. Raghunathan,S., Kozlov,A.G., Lohman,T.M. and Waksman,G. (2000) Structure of the DNA binding domain of *E. coli* SSB bound to ssDNA. *Nat. Struct. Biol*., **7**, 648–652.
32. Bailey,S., Wing,R.A. and Steitz,T.A. (2006) The structure of *T. aquaticus* DNA polymerase III is distinct from eukaryotic replicative DNA polymerases. *Cell*, **126**, 893–904.
33. Gulbis,J.M., Kelman,Z., Hurwitz,J., O'Donnell,M. and Kuriyan,J. (1996) Structure of the C-terminal region of p21(WAF1/CIP1) complexed with human PCNA. *Cell*, **87**, 297–306.
34. Kong,X.P., Onrust,R., O'Donnell,M. and Kuriyan,J. (1992) Three-dimensional structure of the beta subunit of *E. coli* DNA polymerase III holoenzyme: A sliding DNA clamp. *Cell*, **69**, 425–437.
35. Patel,S.S. and Picha,K.M. (2000) Structure and function of hexameric helicases. *Annu. Rev. Biochem*., **69**, 651–697.
36. Song,L., Hobaugh,M.R., Shustak,C., Cheley,S., Bayley,H. and Gouaux,J.E. (1996) Structure of *Staphylococcal* alpha-hemolysin, a heptameric transmembrane pore. *Science*, **274**, 1859–1866.